A Study on Transverse Stability Loss of Planing Craft at Super High Forward Speed

Toru Katayama, *Osaka Prefecture University*

Masashi Fujimoto, *Osaka Prefecture University*

Yoshiho Ikeda, *Osaka Prefecture University*

ABSTRACT

In this study, the mechanism of a transverse stability loss at super high forward speed is investigated. Towing tank test is carried out to observe the characteristics of the instability and it is confirmed that the instability has strong relationship to the change in running attitude and hydrodynamic roll moment due to high forward speed. Using some existing empirical formulas to estimate the dynamic normal force (; lift) on a planing surface, an estimation method of inception of the unstable phenomenon is proposed and its validity is confirmed through comparing with measured results.

Keywords: *Planing Craft, Transverse Stability Loss, Super High Forward speed, Lift*

1. INTRODUCTION

Following the demand of improvement in the speed of a planing craft which exists, if its thrust power is increased, the directional instability with transverse stability loss is often caused. Therefore, in order to secure safety, the elucidation of the cause of occurrence of this instability, the development of the estimation method in a design stage and the proposal of the evasion method are desired.

In this study, the transverse stability loss caused in connection with the directional stability loss is investigated. The transverse stability loss is simulated by a model test and its characteristics are indicated. Fundamental cause of the unstable phenomenon is revealed from the view point of the hydrodynamics. Moreover, an estimation method of occurrence of the unstable phenomenon is proposed.

2. OBSERVATION OF UNSTABLE PHENOMENON BY EXPERIMENT

2.1 Experimental Procedure

Schematic views of experimental setup are shown in Figure 1. A model, which is free in heaving, pitching and rolling, is attached to the high-speed towing carriage through a 3-components load-cell and it is towed horizontally at constant forward speed. Running attitude (; rise, trim angle and heel angle) is measured. In the above-mentioned test, if the model heels over, that indicates the occurrences of the transverse stability loss. As additional test, the measurement of rise and trim angle at rolling fixed to upright condition is also carried out in the same experimental condition, when the model heels over.

In the experiment, two models with different features are used. The body plans are shown in Figure 2. The model M2025, upper side of the

figure, has constant deadrise angle and its form behind the square section number 5.0 is almost prismatic planing surface. On the other hand, another model TB-45 is a deep V monohedron type planing craft and its deadrise angle becomes gradually large ahead. The principle particulars are shown in Table 1.

2.2 Occurrence of Unstable Phenomenon

The measured results of the model M2025 are shown in Figures 3 to 5, and the measured results of the model TB-45 are shown in Figures 7 to 9, respectively. The square mark shows the result when the models are fixed in roll to upright, and the circle mark shows the results when the models are free in roll. Furthermore, the water plane areas for still water surface are obtained from the measured running attitude shown in these figures at roll fixed to upright, and they are shown in Figures 6 and 10.

For the model M2025, the heeling occurs at *Fn*=4.9, and its angle is 7 degrees. The running attitude (rise and trim angle) with the heeling is almost the same as the running attitude without heeling. And the running attitude is continuously changed according to increment of forward speed. Then the water plane area becomes gradually small and narrow triangle according to increment of forward speed.

On the other hand, for the model TB-45, at higher forward speed than *Fn*=2.2, the large heeling occurs and it reaches to 20 degrees. The running attitudes with and without heeling are shown in Figures 7 and 8. And they have large difference. The water plane areas shown in Figure 10 are drastically changed at higher forward speed than *Fn*=2.2 and it becomes narrow pentagon.

For both models, the heeling, which is a transverse instability, is observed at high forward speed range. And the water plane areas of both models become narrow when the instability occurs. From the results, it is supposed that the point of action of the dynamic normal force on planing surface approaches the keel line according to decrement of the water plane breadth and the roll restoring moment is decreased.

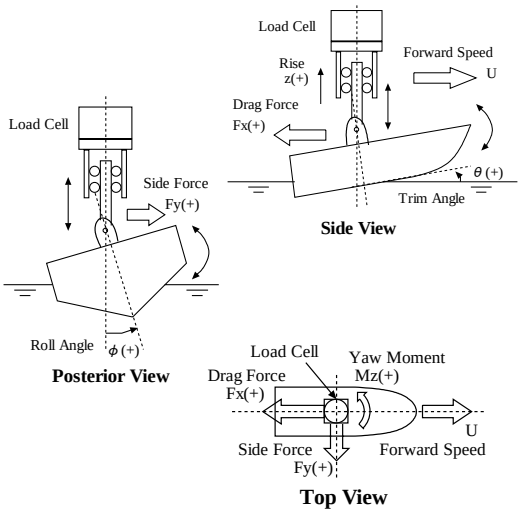

Figure 1 Schematic view of experiment and coordinate system.

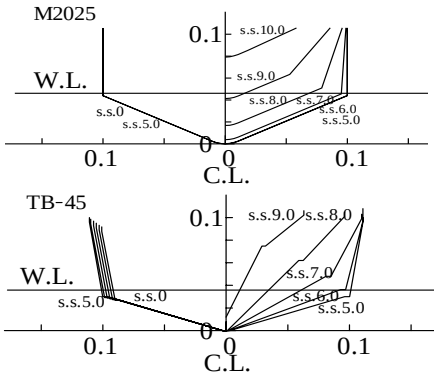

Figure 2 Body Plans of M2025 & TB45.

Table 1 Principal particulars & experimental conditions.

Model	M2025	TB-45
all over length: L_{OA} (m)	0.6	1.0
breadth: B (m)	0.20	0.22
depth: D (m)	0.106	0.102
draft at transom: d_a (m)	0.0403	0.0365
displacement: W (kgf)	2.8	3.1
initial trim angle (degree)	-2.258	0
height of the center of gravity: KG (m)	0.097	0.140
deadrise angle (degree)	25	18
longitudinal towing position from transom (m)	0.240	0.435
height of towing position from Base-Line (m)	0.149	0.075
towing speed (m/sec)	5 - 12	5 - 14

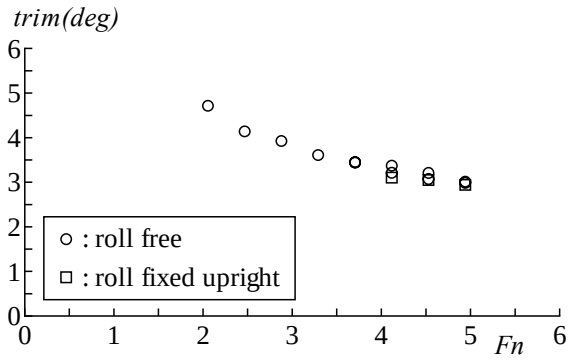

Figure 3 Measured pitching (trim angle) for M2025.

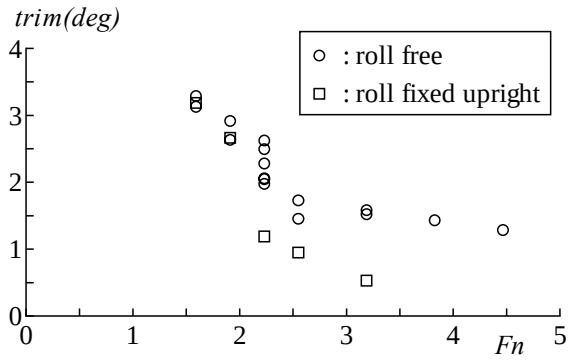

Figure 7 Measured pitching (trim angle) for TB-45.

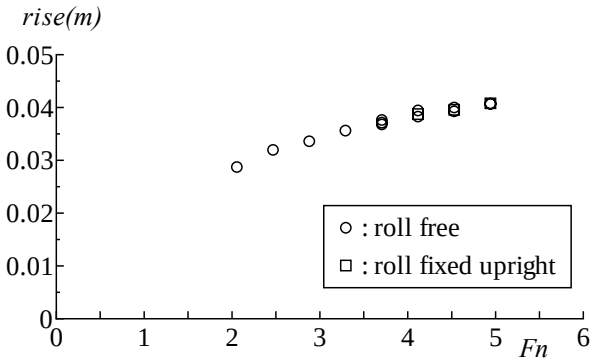

Figure 4 Measured heaving (rise) for M2025.

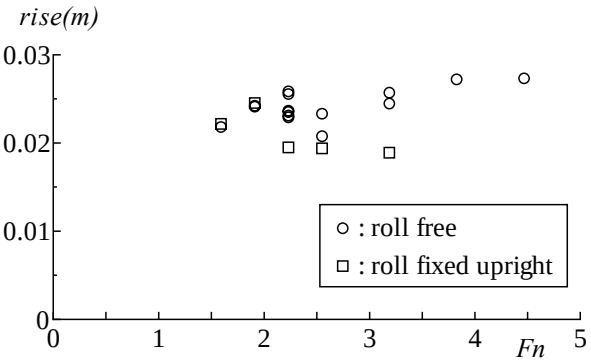

Figure 8 Measured heaving (rise) for TB-45.

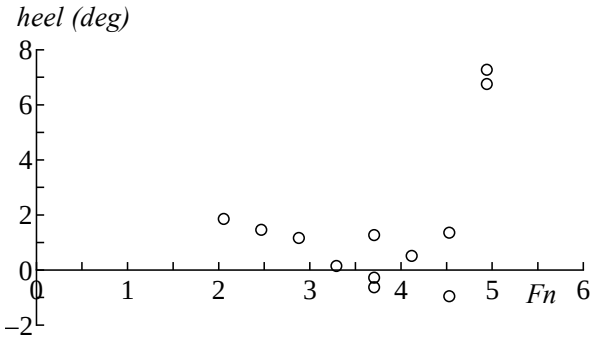

Figure 5 Measured rolling (heel angle) for M2025.

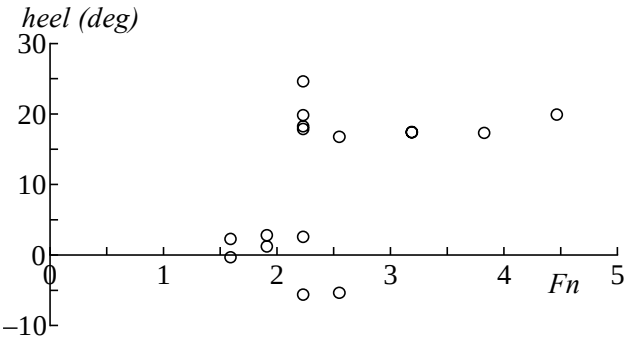

Figure 9 Measured rolling (heel angle) for TB-45.

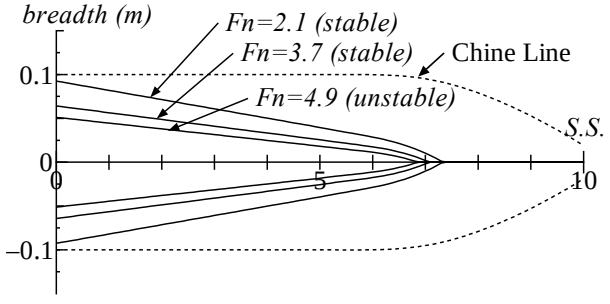

Figure 6 Water plane area for still water surface of M2025 at running condition.

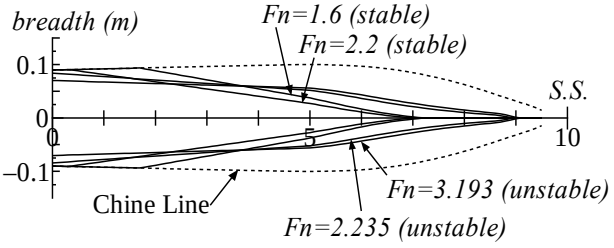

Figure 10 Water plane area for still water surface of TB-45 at running condition.

3. MECHANISM OF INSTABILITY

In the previous paper (Edward M. Lewandowski, 1996), an estimation method of roll restoring moment for planing hull is presented. However, it is difficult to apply the method to the hull shape which has the large difference from prismatic surface because some equations of the method are based on prismatic surfaces (Daniel Savitsky and P. Ward Brown, 1976). In order to ease the limitation, in this paper, based on a strip method, the total roll restoring moment of a 3D V-bottom planing hull is obtained. And the inspection method of transverse stability loss for 3D V-bottom hull is presented.

3.1 Roll Restoring Moment and Instability for 2D V-Bottom Planing Surface

As shown in Figure 11, if a craft has small heeling angle around the center of gravity, the relative deadrise angle to water surface decreases at the planing surface of the heeling side and the dynamic normal force on the side increases, moreover the point of action of the dynamic normal force moves outside. On the other hands, the relative deadrise angle increases at another side and the dynamic normal force on the side decreases, the point of action of the dynamic normal force moves inside. The roll moments caused by the dynamic normal forces on the each side of planing surface are written by the following formulas.

$$\{(cp + \Delta cp_+) - KG\sin\beta\}(N + \Delta N_+) \quad (1)$$

$$(-1)\{(cp - \Delta cp_-) - KG\sin\beta\}(N - \Delta N_-) \quad (2)$$

The next formula is obtained by adding Formulas (1) and (2) and the roll restoring moment caused by hydrostatic pressure.

$$\begin{aligned}&(cp_{x+} - KG\sin\beta_x)N_{x+}\\ &-(cp_{x-} - KG\sin\beta_x)N_{x-} + M_{Bx} = M_x\end{aligned} \quad (3)$$

where

$$\begin{cases} N_{x+} = N_x + \Delta N_{x+} \\ cp_{x+} = cp_x + \Delta cp_{x+} \end{cases} \quad \begin{cases} N_{x-} = N_x - \Delta N_{x-} \\ cp_{x-} = cp_x - \Delta cp_{x-} \end{cases}$$

Equation (3) is the sectional roll restoring moment for 2D V-bottom planing surface.

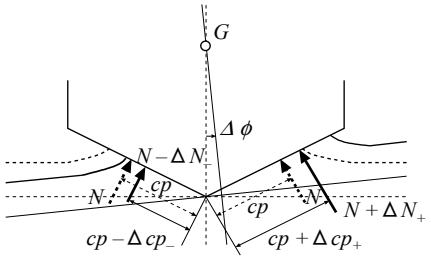

Figure 11 Dynamic normal force on a cross section of V-bottom planing surface with heeling and its point of action.

3.2 Estimation of Transverse Stability Loss for 3D-V Bottom Planing Hull

The roll restoring moment is obtained by integrating with the sectional roll restoring moment expressed by Equation (3).

$$M = \int_A^F M_x dx \quad (1)$$

Moreover, the following equation is obtained by dividing Equation (4) by ship weight W and small heeling angle $\Delta\varphi$.

$$\frac{M}{W \cdot \Delta\varphi} \quad (5)$$

Equation (5) is similar to the slope of *GZ*-curve around upright condition. If it is negative, the craft can not keep upright condition.

In the following part, the ways to calculation of the two terms (cp_x and N_x) in Equation (3) are explained. The position of action of the dynamic normal force on the one side of planing surface is expressed the following equation (Robert. F. Smiley, 1996).

$$cp = E_2 \frac{\pi}{4} c \tag{6}$$

In this equation, E_2 is equal to 0.8 for chines-wet condition, and E_2 is equal to 1.0 for chines-dry condition. And the variables in this equation are shown in Figure 12.

The position of action of the dynamic normal force on the one side of planing surface with small heeling $\Delta\varphi$ around the center of gravity shown in Figure 11 is obtained by substituting c_{x+} or c_{x-} for Equation (6).

$$\begin{aligned} cp_{x+} &= E_2 \frac{\pi}{4} c_{x+} \\ &= \frac{E_2 \pi^2 \{\xi_x + (\cos\Delta\varphi - 1)KG\}}{8\cos\beta_x \cos\Delta\varphi(\tan\beta_x - \tan\Delta\varphi)} \end{aligned} \tag{7}$$

$$\begin{aligned} cp_{x-} &= E_2 \frac{\pi}{4} c_{x-} \\ &= \frac{E_2 \pi^2 \{\xi_x + (\cos\Delta\varphi - 1)KG\}}{8\cos\beta_x \cos\Delta\varphi(\tan\beta_x + \tan\Delta\varphi)} \end{aligned} \tag{8}$$

where ξ_x , β_x , KG are the variables shown in Figure 12.

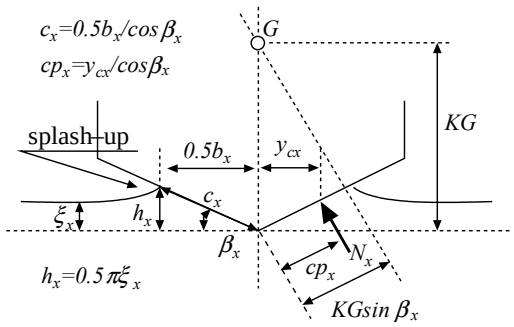

Figure 12 Symbols expressing geometric relations among the water surface, a cross section of planing surface and dynamic normal force on the cross section.

The sectional dynamic normal force on one side of a planing surface per unit length dN/dx is given by the following equation using the sectional dynamic normal force on the keel of a planing surface per unit length dR/dx.

$$\frac{dN}{dx} = \frac{1}{2\cos\beta_x} \frac{dR}{dx} \tag{9}$$

A formula proposed by Peter R. Payne (1996) based on the momentum method is adopted as the sectional dynamic normal force on the keel of a planing surface per unit length.

$$\frac{dR}{dx} = u_0 \cos\tau \frac{d}{dx}\left[m'_x v\right] \tag{10}$$

where u_0 is forward speed, $v(=u_0 \sin\tau)$ is fluid velocity component normal to planing surface, τ is running trim angle. The m'_x is the sectional added mass of a cross-section per unit length, and it is expressed by the next equation.

$$m'_x = C_{m'x} \frac{\pi}{2} \rho \left(\frac{b_x}{2}\right)^2 f(A) \tag{11}$$

$$f(A) = \frac{1}{\sqrt{1+(KA)^2}}$$

$$K = \frac{1}{4} + \sqrt{\frac{2\beta_x}{\pi}}, A = \frac{b^2}{S}$$

where b is chine beam at transom, b_x is a local wetted beam including splash up effects, S is projection of the wetted surface area in the reference plane of a planing surface. $C_{m'x}$ is added-mass coefficient, and it has two different values for chines-wet and chines-dry conditions as the following.

For chines-dry condition:

$$C_{m'x} = \left(1 - \frac{\beta_{Ex}}{2\pi}\right)^2 \tag{12}$$

For chines-wet condition:

$$C_{m'x} = \left(1 + k\frac{z_{cx}}{b_x}\right)\left(1 - \frac{\beta_{Ex}}{2\pi}\right)^2, k = 2 \tag{13}$$

where β_{Ex} in Equations (12) and (13) is called the effective deadrise angle, and it is expressed

as $\tan\beta_{Ex} = \tan\beta_x / \cos\tau$. z_{cx} is chine submergence below the level at which the "splash-up" first wets the chine shown in Figure 13.

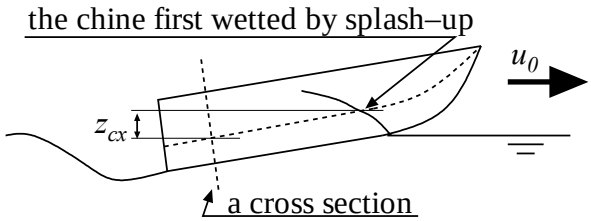

Figure 13 Local chine submergence below the level at which "splash-up" first wets the chine.

The sectional dynamic normal force on one side of a planing surface with small heeling shown in Figure 11 (N_{x+} and N_{x-}) is calculated by substituting b_{x+} , β_{x+} (or b_{x-} , β_{x-}) in Figure 14 and z_{cx+} (or z_{cx-}) with small heeling for Equations (7) to (11).

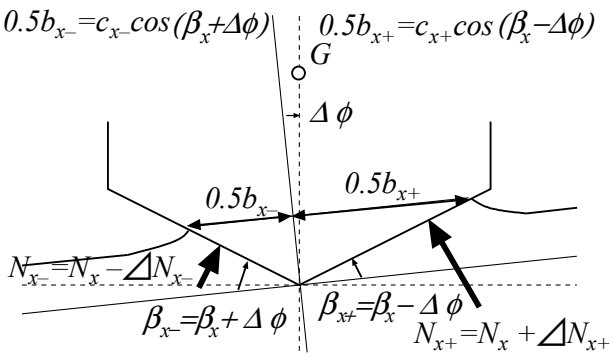

Figure 14 Symbols expressing geometric relations between the water surface and a cross section with small heel.

3.3 Fundamental Cause of Transverse Stability Loss

The estimation results of stability criteria for Model TB-45 and M2025 are shown in Figures 15 and 16, respectively. In Figure 15 for TB-45, two criterions are shown, on the other hand ,in Figure 15 for M2025, one criterion is shown.

The longitudinal distribution of sectional roll restoring moment and the wetted surface area including splash up effects for TB-45 are shown in Figure 17. The figure shows the results at d_a = 0.023 m and τ = 1.0 deg. In this case, the sectional roll restoring moment is negative at the front of the wetted surface and about square section number 2.0. From the investigation of calculation process, it is found that negative at the front is caused by decrement of sectional draft. On the other hand, negative about *S.S.*2.0 is caused by unsymmetrical wetted chine length according to heeling in the case which is chines-wet condition.

In Figure 18, the longitudinal distribution of sectional roll restoring moment and wetted surface area including splash up effects for TB-45 at d_a = 0.011 m and τ = 1.0 deg are shown. And in Figure 19, those for M2025 at τ = 3.0 deg on the stability limit line in Fig.16 are shown. In these figures, both results indicate the same tendency. From the investigation of calculation process of the sectional roll restoring moment, it is found that the negative value of the sectional roll moment is only caused by decrement of sectional draft in the case which is chines-dry condition.

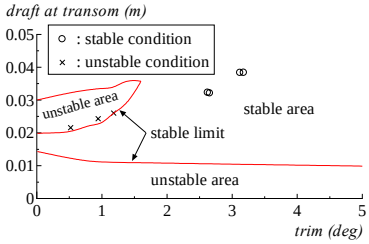

Figure 15 Stable limit for TB-45 shown on running attitude.

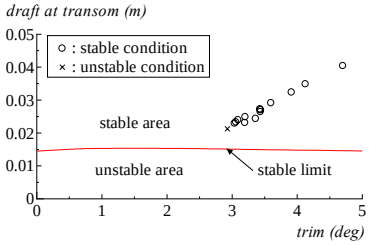

Figure 16 Stable limit for M2025 shown on running attitude.

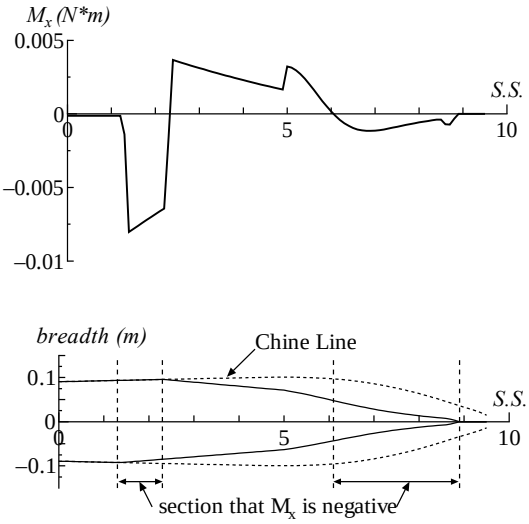

Figure 17 Longitudinal distribution of calculated roll restoring moment and wetted surface area including splash up effects for TB-45 at d_a = 0.023 m and τ = 1.0 deg.

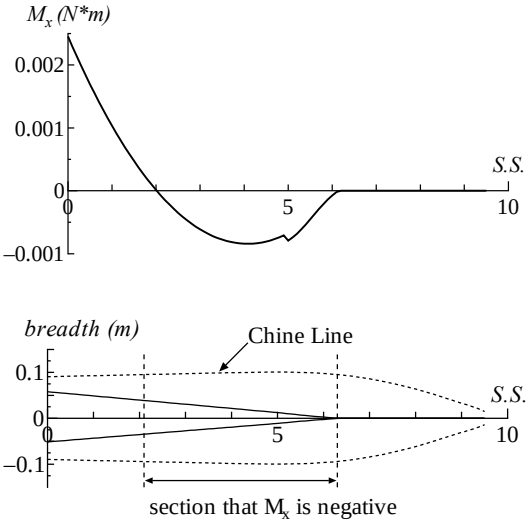

Figure 18 Longitudinal distribution of calculated roll restoring moment and wetted surface area including splash up effects for TB-45 at d_a = 0.011 m and τ = 1.0 deg.

4. CONCLUSIONS

In this study, the fundamental cause of a transverse stability loss at super high forward speed is investigated and the following conclusions are obtained.

1) A transverse stability loss is simulated by

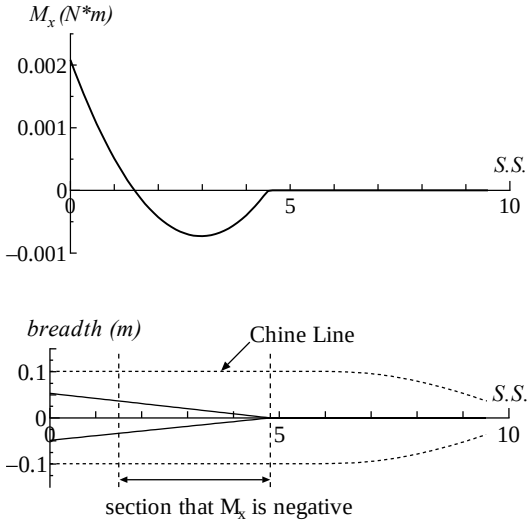

Figure 19 Longitudinal distribution of calculated roll restoring moment and wetted surface area including splash up effects for M2025 at τ = 3.0 deg on the stability limit line in Fig.16.

2) towing tank tests.
3) Using some existing empirical formulas proposed by Robert F. Smiley (1952) and P. R. Payne (1994), it is indicated that the transverse stability loss is caused by change in running attitude according to increment of forward speed.
4) An estimation method of its stability criteria is proposed.

Using the estimation method proposed in this study, it is found that there are two unstable regions, for a conventional deep V monohedron planing craft, depending hull form.

5. REFERENCES

Robert F. Smiley, 1952, “A Theoretical and Experimental Investigation of the Effects of Yaw on Pressures, Forces, and Moments during Seaplane Landing and Planing”, NACA Technical Note 2817.

Edward M. Lewandowski, 1996, “Prediction of the Dynamic Roll Stability of Hard-Chine Planing Craft”, Journal of Ship Research, Vol.40, No.2, pp.144-148.

P. R. Payne, 1994, “Recent Developments in “Added-Mass” Planing Theory”, Ocean Engineering, Vol.21, No.3, pp.257-309.

Daniel Savitsky and P. Ward Brown, 1976, “Procedures for the Hydro Evaluation of Planing Hulls in Smooth and Rough Water”, Marine Technology, Vol.13, No.4, pp.381-400.